Crystal structure of tubulin tyrosine ligase-like 3 reveals essential architectural elements unique to tubulin monoglycylases

Christopher P. Garnham[a], Ian Yu[a], Yan Li[b], and Antonina Roll-Mecak[a,c,1]

[a]Cell Biology and Biophysics Unit, Porter Neuroscience Research Center, National Institute of Neurological Disorders and Stroke, Bethesda, MD 20892; [b]Mass Spectrometry Core, Porter Neuroscience Research Center, National Institute of Neurological Disorders and Stroke, Bethesda, MD 20892; and [c]National Heart, Lung, and Blood Institute, Bethesda, MD 20892

Edited by David Baker, University of Washington, Seattle, WA, and approved April 26, 2017 (received for review October 21, 2016)

Glycylation and glutamylation, the posttranslational addition of glycines and glutamates to genetically encoded glutamates in the intrinsically disordered tubulin C-terminal tails, are crucial for the biogenesis and stability of cilia and flagella and play important roles in metazoan development. Members of the diverse family of tubulin tyrosine ligase-like (TTLL) enzymes catalyze these modifications, which are part of an evolutionarily conserved and complex tubulin code that regulates microtubule interactions with cellular effectors. The site specificity of TTLL enzymes and their biochemical interplay remain largely unknown. Here, we report an in vitro characterization of a tubulin glycylase. We show that TTLL3 glycylates the β-tubulin tail at four sites in a hierarchical order and that TTLL3 and the glutamylase TTLL7 compete for overlapping sites on the tubulin tail, providing a molecular basis for the anticorrelation between glutamylation and glycylation observed in axonemes. This anticorrelation demonstrates how a combinatorial tubulin code written in two different posttranslational modifications can arise through the activities of related but distinct TTLL enzymes. To elucidate what structural elements differentiate TTLL glycylases from glutamylases, with which they share the common TTL scaffold, we determined the TTLL3 X-ray structure at 2.3-Å resolution. This structure reveals two architectural elements unique to glycyl initiases and critical for their activity. Thus, our work sheds light on the structural and functional diversification of TTLL enzymes, and constitutes an initial important step toward understanding how the tubulin code is written through the intersection of activities of multiple TTLL enzymes.

tubulin code | TTLL enzymes | glycylation | tubulin modification | glutamylation

Microtubules are multifunctional dynamic polymers essential in eukaryotic cells. Their basic building block is the α/β-tubulin heterodimer. It consists of a compact folded tubulin body and intrinsically disordered C-terminal tails. These tails form a dense lawn on the microtubule surface and serve as binding sites for molecular motors and microtubule-associated proteins (1). Tubulin tails are functionalized with abundant and chemically diverse posttranslational modifications that constitute an evolutionarily conserved tubulin code that specializes microtubule subpopulations in cells and tunes their interaction with effectors (2–6). The majority of these modifications are catalyzed by a phylogenetically widespread family of homologous enzymes whose members include tubulin tyrosine ligase (TTL) and multiple TTL-like (TTLL) enzymes that add either tyrosine, glutamate, or glycine to the tubulin tails (7–13) (reviewed in ref. 3). Understanding the structure and biochemical characteristics of these enzymes is essential to deciphering the tubulin code, as it is their collective action that gives rise to the stereotyped microtubule modification patterns observed in cells. Some of the most heavily modified microtubules are in the axonemes of cilia and flagella, organelles with critical roles in cell signaling, directed fluid flow, and cell motility (14, 15). Axonemal microtubules are particularly enriched in glycylation and glutamylation. Whereas glutamylation is found on both cytoplasmic and axonemal microtubules, glycylation is found almost exclusively in axonemes and thus thought to specifically tune microtubule functions in this specialized organelle (3).

Glycylation is the ATP-dependent addition of glycines, either singly or in chains, to internal glutamates (16). Tubulin glycylation is conserved in protists and most metazoans (17). The glycyl chain length on either α- or β-tubulin tails in axonemes is highly variable (16–18), ranging from 1 to 40 posttranslationally added glycines (19). Of the 13 TTLL enzymes in mammals (10, 11), three are glycylases: TTLL3, -8, and -10 (12, 13, 20). Cellular overexpression studies suggest that these enzymes are specialized for either initiating (TTLL3 and TTLL8) or elongating the glycyl chain (TTLL10) (12, 20). Such specialization would not be surprising, as initiation requires the enzyme to accommodate a glutamate and an incoming glycine in its active site and catalyze formation of an isopeptide bond, whereas elongation requires it to accommodate two glycines and catalyze a standard peptide bond.

Glycylation is critical for the stability of primary (21) and motile cilia (22). TTLL3 loss decreases numbers of ciliated colon epithelial cells (21), and loss of both TTLL3 and -8 reduces primary cilia stability and leads to motile cilia loss (22). In mice, loss of TTLL3-mediated glycylation in colon epithelial cells results in increased cell proliferation and the potentiation of cancerous cell growth (21). Consistent with this phenotype, TTLL3-inactivating mutations have been identified in colon cancer patients (12, 23). Glycylation is also important during development. Knockdown of TTLL3 in developing zebrafish embryos causes pronephric kidney

Significance

Tubulin is subject to diverse posttranslational modifications that constitute a code read by cellular effectors. Most of these modifications are catalyzed by tubulin tyrosine ligase-like (TTLL) family members. The functional specialization and biochemical interplay between TTLL enzymes remain largely unknown. Our X-ray structure of TTLL3, a tubulin glycylase, identifies two functionally essential architectural elements and illustrates how the common TTL scaffold was used to functionally diversify the TTLL family. We show that TTLL3 competes with the glutamylase TTLL7 for overlapping modification sites on tubulin, providing a molecular basis for the anticorrelation between these modifications observed in vivo. Our results illustrate how a combinatorial tubulin code can arise through the intersection of activities of TTLL enzymes.

Author contributions: C.P.G., I.Y., Y.L., and A.R.-M. designed research; C.P.G., I.Y., and Y.L. performed research; C.P.G., I.Y., Y.L., and A.R.-M. analyzed data; and C.P.G. and A.R.-M. wrote the paper.

The authors declare no conflict of interest.

This article is a PNAS Direct Submission.

Data deposition: Atomic coordinates and structure factors reported in this paper have been deposited in the Protein Data Bank, www.pdb.org (PDB ID code 5VLQ).

[1]To whom correspondence should be addressed. Email: antonina@mail.nih.gov.

This article contains supporting information online at www.pnas.org/lookup/suppl/doi:10.1073/pnas.1617286114/-/DCSupplemental.

cysts, randomized multicilia orientation, and defects in ciliary fluid flow (13, 24), whereas knockout of TTLL3B is lethal in flies (12).

All glycylase studies have been so far performed in vivo (13, 24). Their mechanistic interpretation is complicated by their apparent functional redundancy and the complexity of microtubule modifications in vivo. Thus, despite the importance of glycylation in regulating basic cellular processes, a biochemical and structural framework to understand the activities of TTLL glycylases is lacking. Here we focus on the mechanistic dissection of TTLL3 and show that it strictly initiates glycyl chains on the β-tubulin tail using a positional hierarchy. Moreover, we find that TTLL3 competes with the glutamylase TTLL7 for overlapping modification sites on the β-tail, providing a molecular basis for the anticorrelation between glutamylation and glycylation observed in vivo (12, 25, 26). Consistent with this competition for modification sites, TTLL3 activity is reduced on glutamylated versus unmodified microtubules. Surprisingly, we find that TTLL3 can switch substrate preference in a glutamylation-dependent manner. Finally, to understand what architectural elements distinguish TTLL glycylases from glutamylases, we determined the X-ray crystal structure of TTLL3 to 2.3-Å resolution. This structure revealed two structural elements and a sequence motif unique to glycyl initiases that we show are critical for their activity.

Results

TTLL3 Preferentially Initiates Glycyl Chains on β-Tubulin Tails Following a Positional Hierarchy. Cellular studies using antibodies that recognize monoglycylated tubulin indicate that TTLL3 is a glycyl chain initiator capable of modifying both α- and β-tubulin (12, 13). We find that recombinant TTLL3 preferentially glycylates a β-tail peptide over the α-tail (Fig. 1*A*). This preference also holds with microtubules (Fig. 1*B* and Fig. S1), indicating that the TTLL3 active site is specific for the β-tail. At higher enzyme-to-substrate ratios or longer incubations, the α-tubulin tail is minimally modified by TTLL3, indicating that this specificity is limited, consistent with cellular overexpression studies showing glycylation of both α- and β-tubulin (12).

We then mapped glycylation sites on TTLL3-modified microtubules using tandem mass spectrometry (MS/MS). We used as substrate microtubules assembled from unmodified human tubulin purified via an affinity method from tSA201 cells (27, 28) (*SI Materials and Methods*). We monitored reaction progression by LC/MS (Fig. 1 and Fig. S1*B*). The LC/MS analysis showed a gradual depletion of the unmodified species concomitant with an increase in the monoglycylated species, and at longer time points the conversion from lower- to higher-order glycylated species with as many as four added glycines (Fig. 1*C*). Mapping of TTLL3 glycylation sites on the βI-tail [βI is one of the two major β-tubulin isoforms in tSA201 cells and also found in axonemal microtubules (29)] revealed a hierarchy of modification sites (Fig. 1 and Fig. S2). The primary modification site is E441 (Fig. S2 *A* and *E*). This site is followed by E438 and E442, yielding two diglycylated species of roughly equal abundance as revealed by extracted-ion chromatograms (XICs) (Fig. S2 *B* and *F*), followed by E439 (Fig. 1 and Fig. S2*C*). MS/MS, MS/MS/MS, as well as electron transfer dissociation experiments did not detect elongated glycine chains even at extended incubation times and higher enzyme:substrate ratios, indicating that TTLL3 is indeed a glycyl chain-initiating enzyme (*SI Materials and Methods*). The TTLL3-modified sites we identify concentrate on the last five glutamates in βl, previously found to be glycylated in β-tubulin isolated from *Paramecium tetraurelia* (30) and *Purpurus lividus* (31).

TTLL3 and 7 Target Overlapping Glutamates in the β-Tubulin Tail. Competition for substrate between glutamylases and glycylases has been proposed as a regulatory mechanism (13, 26, 32) because inhibition or overexpression of glutamylases causes marked increases or decreases in glycylation and vice versa (13). To test this hypothesis, we used MS/MS to sequence the βI-tubulin tails from microtubules glutamylated by TTLL7, a β-tubulin–specific glutamylase that initiates and elongates glutamate chains (33). Both TTLL3 and TTLL7 localize to cilia (10, 13). These MS/MS

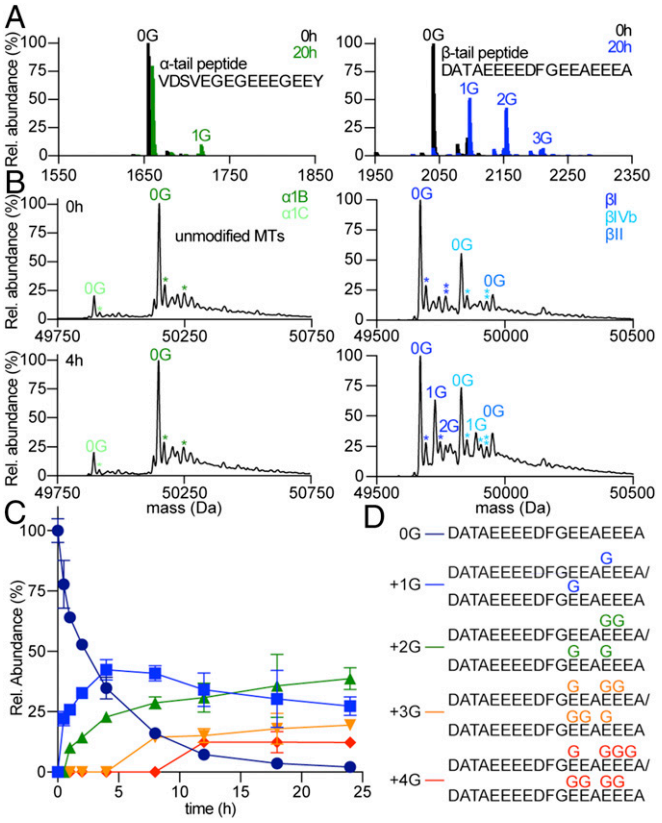

Fig. 1. TTLL3 is a glycylation-initiating enzyme that modifies the β-tubulin tail. (*A*) Deconvoluted mass spectra of a synthetic C-terminal α1B- (*Left*) and βI-tubulin peptide (*Right*) glycylated by TTLL3 at a 1:20 enzyme:peptide molar ratio. Unmodified peptides at *t* 0 h, black; peaks corresponding to glycylated products, green and blue for α1B and βI, respectively. The Gly number added to each species is indicated. (*B*) Deconvoluted α- and β-tubulin mass spectra of Taxol-stabilized human microtubules (MTs) glycylated by TTLL3 at a 1:20 enzyme:tubulin molar ratio. The Gly number added is indicated and colored according to isoform. * and ** indicate Na^+ and $(N_2FeOH)^{1+}$ adducts generated during LC/MS, respectively (46). (*C*) Reverse-phase LC/MS of TTLL3-modified human naïve microtubules tracking the normalized *m/z* intensity of individual βI-tubulin glycylated species over time (*SI Materials and Methods*). Mean ± SEM ($n = 3$). (*D*) Hierarchy of TTLL3 glycylation on the βI-tubulin tail from MS/MS experiments (*Materials and Methods*).

experiments are challenging, because the high glutamate numbers in the tubulin tails make it hard to distinguish between main-chain and posttranslationally added glutamates in fragmentation patterns. To overcome this problem, we used heavy, [^{13}C]Glu as substrate for TTLL7 (*SI Materials and Methods*). We found two main glutamylation sites in βI: E434 and E441 (Fig. 2*A* and Fig. S3 *B* and *C*). E442 and E443 were also modified, but with much lower frequency (<1% as determined from XICs). Thus, our MS/MS experiments indicate that TTLL3 competes with TTLL7 for its main modification site E441 (Fig. 2 *A* and *B*).

Tubulin used in most biochemical studies is isolated from brain tissue because of its abundance and ease of purification. This tubulin is diversely posttranslationally modified and especially enriched in polyglutamylation [average Glu number ranging from 3 to 6 with as many as 11 and 7 on α- and β-tails, respectively (34)]. E441, the primary site modified by TTLL3, is glutamylated in mouse brain tubulin (35). Consistent with this finding, TTLL3 is 75% less active with heterogeneous brain microtubules compared with unmodified human microtubules (Fig. 2*C*). We next systematically investigated the effect of glutamylation on TTLL3 glycylation by performing activity assays with microtubules with quantitatively defined glutamylation levels generated through in vitro enzymatic modification of unmodified human microtubules using TTLL7 (4)

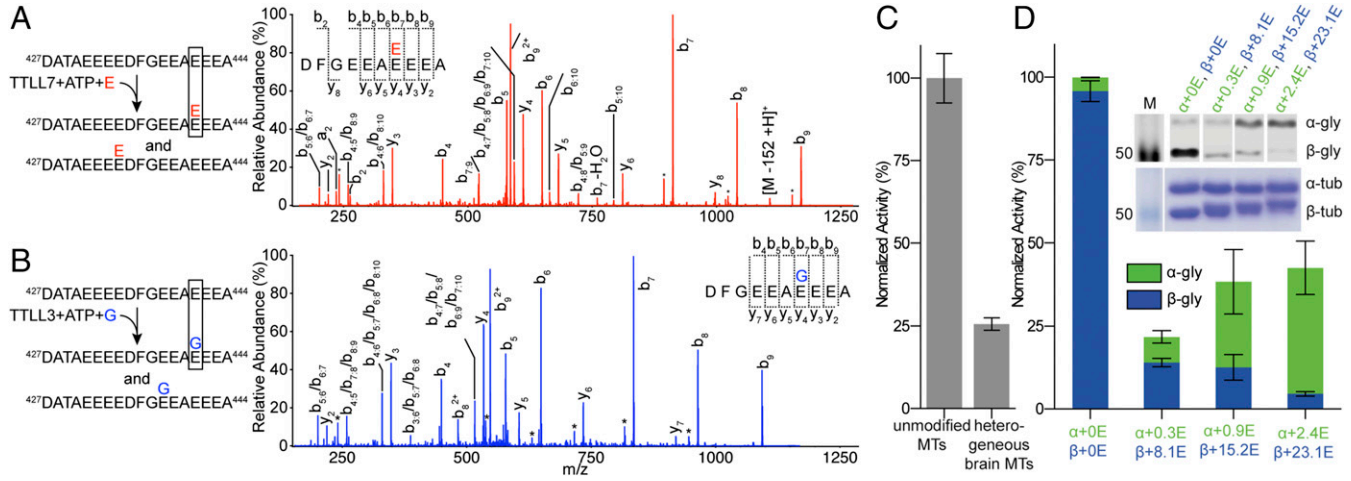

Fig. 2. TTLL3 and TTLL7 compete for overlapping sites on the β-tubulin tail. (*A*) MS/MS spectrum of a βI-tubulin tail peptide fragment proteolytically released from microtubules glutamylated by TTLL7 showing glutamylation at E441. Individual a-, b-, and y-series ions for each spectrum are shown together with the deduced sequence. Asterisks indicate ions with neutral loss of an H_2O group. The annotation i:j represents a fragment from internal cleavage; for example, b4:7 represents the peptide fragment from the fourth to the seventh residue. All possible species are listed when different fragments have the same mass. (*B*) MS/MS spectrum of a βI-tubulin tail peptide fragment proteolytically released from microtubules glycylated by TTLL3 showing glycylation at E441 (annotated as in *A*). (*C*) Normalized glycylation activity of TTLL3 on unmodified and heterogeneous brain microtubules. Mean ± SEM ($n = 3$). (*D*) Normalized TTLL3 glycylation activity of TTLL3 on unmodified and glutamylated microtubules. Mean ± SEM ($n = 2$). The weighted average of glutamates added to α- and β-tubulin is indicated. (*D*, *Inset*) Western blot of the 3-h time point of each reaction probed with the monoglycylation-specific TAP952 antibody (*Top*) and Coomassie-stained SDS/PAGE of glutamylated microtubules used as substrates (*Bottom*).

(Fig. 2*D* and *SI Materials and Methods*). TTLL3 glycylation was reduced by 86% with microtubules carrying a weighted average <E> of 8.1 glutamates on their β-tails compared with unmodified microtubules. Further increase in glutamylation levels (<E> 15.2 and 23.1, respectively) resulted in only a modest decrease in β-tubulin glycylation (87 and 95%, respectively). This leveling off is likely due to a saturation of TTLL3 modification sites by TTLL7 and the fact that the additional glutamates added at higher glutamylation levels are on non-TTLL3 sites. These results show a direct competition between a TTLL glutamylase and glycylase for the same modification sites on tubulin and provide a mechanistic explanation for the anticorrelation between these modifications observed in vivo.

Interestingly, TTLL3 gradually switches to modify the α-tail as β-tubulin glutamylation levels increase and presumably the TTLL3 initiation sites on this tail have already been glutamylated: α-Tubulin glycylation increases ∼10-fold on microtubules with higher glutamylation levels (α+2.4E, β+23.1E) (Fig. 2*D*). TTLL3 localizes to axonemes. These cellular structures contain the highest levels of glutamylation reported in vivo (as many as 21 glutamates) (36, 37). Moreover, in vivo studies indicate that most glycylation on ciliary microtubules occurs after glutamylation, with glyclation being required for cilia maintenance and glutamylation for their biogenesis (22). Our data demonstrate that TTLL3 can display glutamylation-dependent tubulin-tail preference.

TTLL3 Crystal Structure: A Variation on the TTL Theme. The structure of the glutamylase TTLL7 (38) revealed how sequence elements specific to glutamylases differentiate the conserved TTL scaffold (39, 40). To elucidate what architectural features specialize the TTL fold for glycylation, we determined the X-ray crystal structure of the conserved core of *Xenopus tropicalis* TTLL3 (residues 6–569) bound to the slowly hydrolyzable ATP analog AMPPNP (Fig. 3 and Fig. S4) using single-wavelength anomalous dispersion (*Materials and Methods*). This core construct is active (2.7 ± 0.2 Gly per h) and its activity is comparable to the full-length enzyme (Fig. S4*D* and *SI Materials and Methods*). The structure was refined at 2.3-Å resolution to an R_{free} of 23.0% (Table S1). Two molecules of TTLL3 are present in the asymmetric unit of our crystals (Fig. S4*B*); however, size-exclusion chromatography shows the protein is monomeric in solution (Fig. S4*C*). Structural variation between the two chains is low (rmsd 0.29 Å over all C_α atoms; Fig. S4*E*). TTLL3 is elongated (∼94 × 47 × 23 $Å^3$) and composed of an N (residues 6–138), central (residues 139–377), and C domain (residues 378–569) (Fig. 3*A*). A central mixed-polarity β-sheet supports the active site, which lies at the junction of the three domains. The C-domain strand β13 reaches into the N domain and bridges the β-sheets in these domains to form a continuous, highly curved β-sheet that bisects TTLL3. The nucleotide is wedged between the central and C domains (Fig. 3*A*). Despite the presence of AMPPNP in our crystals, the γ-phosphate is not well-localized, possibly because of the absence of the tubulin substrate, as seen previously for TTLL7 (38) (Fig. S4*F*).

The TTLL3 core is structurally homologous to TTL (40) (all-C_α rmsd 1.7 Å; Fig. 3 *A* and *D*). However, TTLL3 has two additional structural elements, designated IS1 and IS2 (Fig. 3 and Fig. S5). IS1 is composed of two helices, α1 and α3, the first an N-domain extension and the latter an insertion between β2 and β3 (Fig. 3 *A* and *D* and Fig. S5). α3 is stabilized by knobs-in-holes apolar interactions with α1 and β2 of the N domain (Fig. 3*C*). IS2 is a 138-residue insertion that extends the central-domain helix α5 and completes a four-helix bundle comprising α5 through α8 (Fig. 3 *A* and *B* and Fig. S5). Helices α6, -7, and -8 of IS2 are stabilized through extensive hydrophobic interactions: Invariant W281 of α7 stacks against W188 of α5; invariant Y288 and Y289 of α7 make van der Waals and polar contacts with α5, α9, and the α8–β6 loop (Fig. 3*B*). Both IS1 and IS2 are critical for TTLL3 activity (see below). The TTLL3 structure is distinct from that of the glutamylase TTLL7, composed of the TTL core augmented by an α-helical cationic microtubule-binding domain (Fig. 3*E*) (38).

Molecular Determinants for Microtubule Recognition by TTLL3. The TTLL3 molecular surface displays two conserved positively charged interconnected regions: one extending from the ATP binding site to the N-, central-, and C-domain junction, and the second from the tip of IS1 to the posterior surface of the C domain (Fig. 4 *A* and *B*). This extended surface is likely a site of interaction with the negatively charged tubulin tails and microtubule surface. The active site is lined with basic residues conserved in all TTL and TTLL enzymes. Invariant R411 stabilizes the ATP γ-phosphate in TTL (39, 40) (Fig. 4 *A* and *C*). R389 is also invariant. Its equivalent residue in TTL coordinates the tubulin-tail glutamate that ligates to the incoming

BIOCHEMISTRY

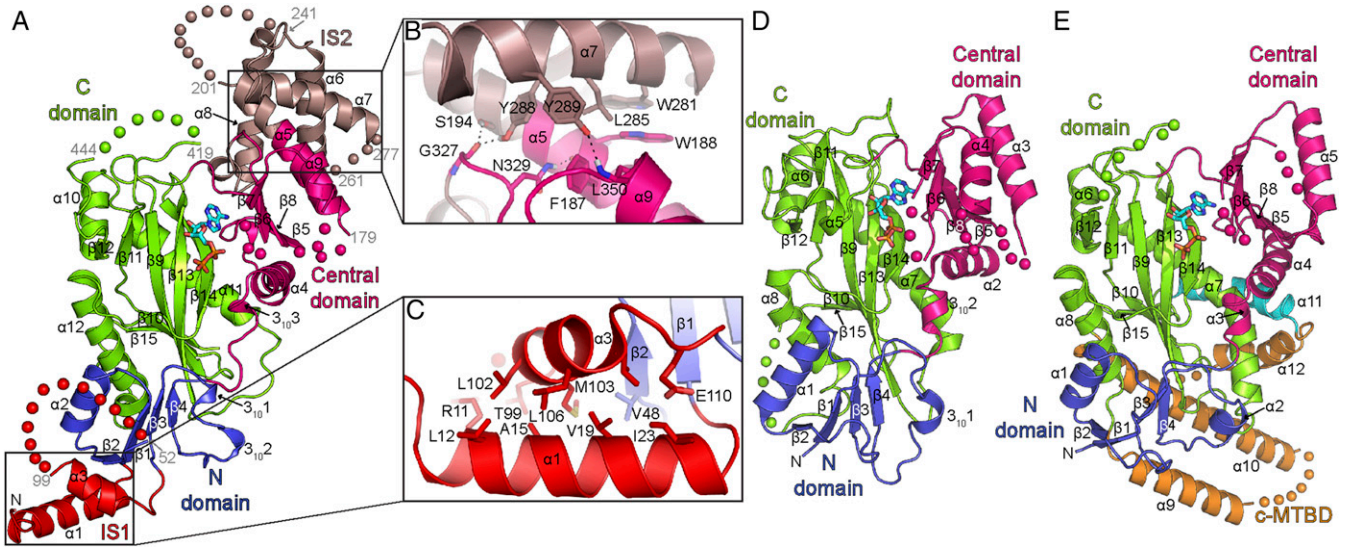

Fig. 3. TTLL3 crystal structure and comparison across the TTLL family. (*A*) Cartoon representation of the TTLL3 core bound to AMPPNP. (*B*) Close-up of the interface between IS2 α7 and central domain α5. (*C*) Close-up showing interactions between IS1 α1 and α3. (*D*) X-ray crystal structure of TTL [Protein Data Bank (PDB) ID code 4IHJ]. (*E*) Hybrid X-ray and cryo-EM structure of TTLL7 [PDB ID code 4YLS, Electron Microscopy Data Bank (EMD) ID code EMD-6307]; the cMTBD atomic model (gold) is based on the EM map and is incomplete. Nucleotides are in ball-and-stick format. Spheres indicate disordered segments.

tyrosine (39). Consistent with their importance in substrate binding, R389E and R411E mutations in TTLL3 reduce glycylation to background levels (Fig. 4*D*). Interestingly, G505 (G597 in humans) is mutated to serine in colorectal cancer patients (12, 23, 41). This mutation would cause a steric clash with R389, likely affecting ATP binding. Another disease mutation is M527I (M619 in humans). This residue is involved in conserved hydrophobic interactions that stabilize the α12–β14 loop that wraps the active site (Figs. 3*A* and 4 *A* and *B*). Both disease mutations inactivate TTLL3 (12).

Conserved K119, R126, and K139 located toward the N- and central-domain interface are important for substrate recognition, as their mutation decreases activity dramatically (Fig. 4 *C* and *D*). Previous studies established this surface as important for tubulin-tail recognition by TTL (40) and TTLL7 (38), and it thus likely constitutes the binding platform for the tubulin tail in TTLL3 also. Because these surface residues are >20 Å from the active site, they are likely involved primarily in substrate binding and not chemistry. Invariant S142 is also in this region. MS/MS sequencing of our recombinant TTLL3 revealed it was partially phosphorylated during expression in insect cells (*SI Materials and Methods*). In vitro dephosphorylation increased activity approximately twofold, as did mutation to Ala, whereas a phosphomimetic S142D mutation reduced activity to background (Fig. 4*D*). Thus, phosphorylation at this site could potentially regulate TTLL3. This serine is in a weak consensus site for PKA and PKC (42).

The convex ridge of TTLL3 running from the tip of IS1 α1 to the N- and central-domain junction is studded with conserved positively charged residues likely involved in microtubule binding (Fig. 4*C*). Consistent with their high degree of conservation, double mutation of K13A K16A and K24A K26A leads to 61 and 96% lower glycylation, respectively (Fig. 4*D*). Single charge-reversal mutation of invariant K130, R556, and K568 reduces activity by

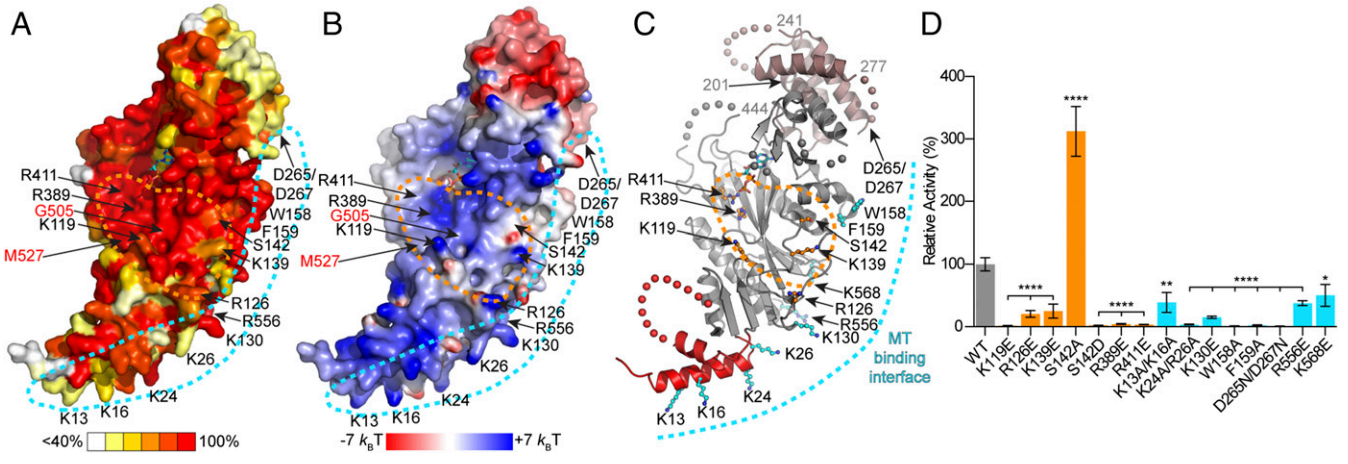

Fig. 4. Molecular determinants of microtubule glycylation by TTLL3. (*A*) TTLL3 molecular surface colored according to conservation (red, 100% identity; white, <40%). (*B*) TTLL3 molecular surface colored according to electrostatic potential (red, negative; blue, positive; from −7 to +7 k_BT). IS2 residues D265–D267 are not resolved in our structure. (*C*) TTLL3 structure showing residues important for glycylation. Residues at the proposed microtubule-binding interface are shown in aqua; those in the active site and tubulin tail-binding groove are shown in orange. IS1 and IS2 are in red and violet, respectively. Disordered regions are shown as spheres. (*D*) Normalized in vitro glycylation activity of recombinant structure-guided TTLL3 mutants with unmodified human microtubules. Activity was measured by Western blot using the TAP952 anti-monoglycylated tubulin antibody (*SI Materials and Methods*). *P < 0.05, **P < 0.01, and ****P < 0.0001. Mean ± SEM ($n \geq 6$).

85, 63, and 50% compared with wild type, respectively. This positively charged ridge is bordered by a hydrophobic patch formed by invariant W158 and F159 (Fig. 4*C* and Fig. S6) that are solvent-exposed and likely also involved in substrate interactions. Their mutation reduces activity by 98 and 97%, respectively (Fig. 4*D*).

Glycyl Initiases TTLL3 and 8 Share Common Architectural Elements Critical for Activity. TTLL3 is conserved from ciliated protists to humans (Fig. S5) and most closely related to TTLL8, also a glycyl chain-initiating enzyme (12). The enzymatic cores of the two proteins are ∼49% identical (68% similarity; Fig. S5), with both surface as well as hydrophobic core residues strongly conserved (Fig. 5*A* and Fig. S7*B*). Our structure-based sequence analysis shows that TTLL8 contains both IS1 and IS2, and the TTL core surfaces that interact with these elements are conserved (Fig. 3 *B* and *C* and Figs. S5 and S7 *A* and *B*). Structure-based bioinformatic analysis did not uncover these elements in any other TTLL family member. TTLL3 has lower overall similarity to TTLL10 (25% identity, 45% similarity), the only TTLL enzyme thought to be a glycine-chain elongator. Importantly, IS1 and IS2 are absent in TTLL10. Thus, our structural and functional analyses demonstrate that IS1 and IS2 are defining structural elements of TTLL enzymes that initiate glycyl chains.

All key residues important for TTLL3 activity are conserved in TTLL8s (Fig. 5 and Figs. S5 and S7), including residues that line the proposed tubulin tail (K185, H192, K205, and S208) and microtubule-binding interfaces (K93, R96, K104, R106, W224, Y225, R619, and R631). Charge-reversal mutation of K185, H192, and K205 in TTLL8 reduces its activity in cells by 98, 64, and 93% of wild-type levels, respectively (Fig. 5*B*). Residues on the positively charged microtubule-binding ridge are also strongly conserved between TTLL3 and -8. Double charge-reversal mutations K93E R96E and K104E R106E both reduce activity by 99%, whereas single mutations R619E and R631E reduce activity by 75 and 74%, respectively. As in TTLL3, this positively charged ridge is flanked by a conserved hydrophobic patch containing invariant W224 and Y225. Their mutation reduces glycylation dramatically (Fig. 5*B*).

The flexible loop connecting α6 and α7 of IS2 extends the convex interaction ridge on TTLL3. It contains a conserved DID sequence motif (Fig. 5*C*) present in all TTLL3s and 8s but absent in TTLL10 enzymes, consistent with a specialization for glycyl initiases. Mutation of the two conserved aspartates (D265N D267N) reduces glycylation by 98% in vitro (Fig. 4*D*), and human bone osteosarcoma epithelial cells (U2OS) expressing this mutant show no detectable glycylation (Fig. 5*D*). Mutation of this motif in TTLL8 (D328N D330N) reduces activity to 20% of wild-type levels (Fig. 5*B*). Thus, this signature sequence motif is critical for the activity of TTLL glycyl initiases.

Discussion

Our in vitro characterization reveals that the TTLL3 glycylase adds single glycines to multiple sites on the β-tail following a positional hierarchy, with E441 as the main modification site. TTLL3 shows preference for the β-tail either in isolation or presented in the microtubule context. The TTLL3 mechanism of substrate recognition differs from the glutamylase TTLL7. In the case of TTLL7, preferential modification of the β-tail arises from additional interactions with the microtubule distant from the active site (38). Cellular studies indicate that TTLL8 is an α-tubulin–specific initiase (12, 20). Thus, there are two glycyl initiases in mammals, TTLL3 and -8, whereas TTLL10 functions as an elongase adding multiple glycines on both α- and β-tails (12, 20). Interestingly, no polyglycylated tubulin was found in humans (12, 17). This lack of polyglycylation was proposed to be due to two inactivating mutations in human TTLL10 (N448S and T467K) (12). Surprisingly, our structure reveals that these mutations map to α10 and α11 on the enzyme posterior surface, away from the active site (Fig. S5), where they are unlikely to have a direct effect on activity.

Our TTLL3 crystal structure identifies unique architectural elements that define a TTLL member as an initiating glycylase. TTLL3 augments its TTL-like core with two conserved elements, IS1 and IS2, critical for glycylation (Fig. 3). These architectural extensions reside at opposite ends of a positively charged microtubule recognition interface (Fig. 4) and are distinctly different from the cationic α-helical microtubule-binding domain (cMTBD) shared among autonomous glutamylases (Fig. 3) (38). The cMTBD is absent from glycylases (Fig. S8). Thus, our work reveals a second strategy for functionalizing the TTL structural scaffold to achieve substrate recognition diversity in the family.

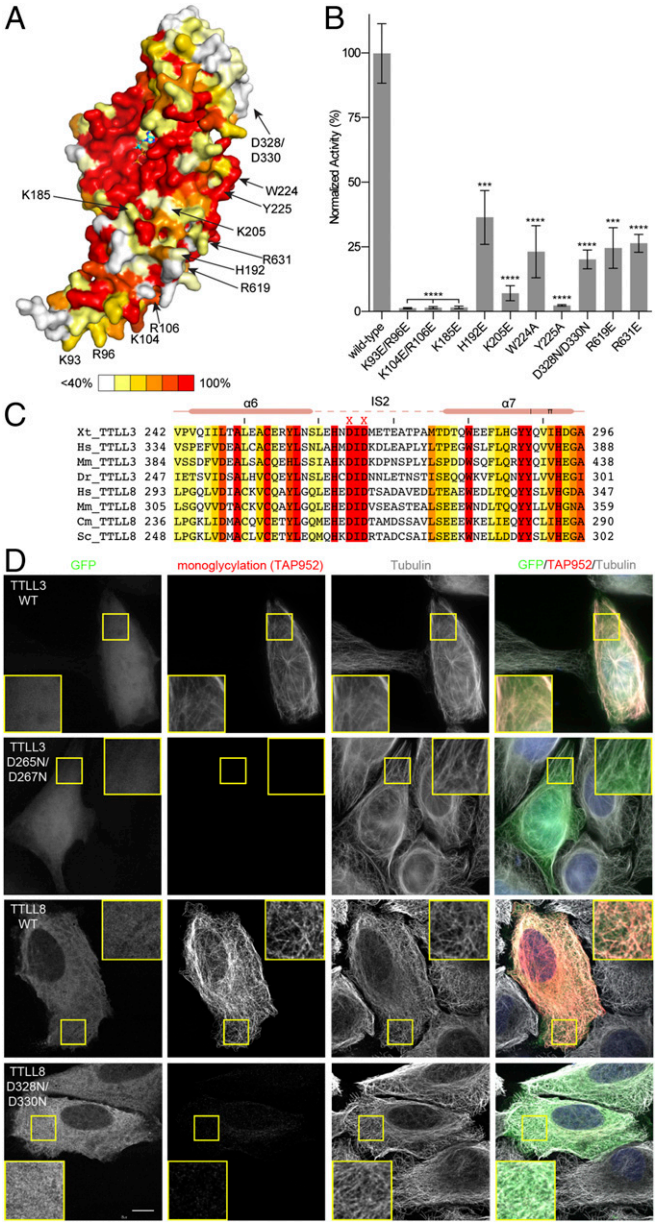

Fig. 5. TTLL3 and TTLL8 share structural elements critical for glycylation. (*A*) The TTLL3 molecular surface is colored according to conservation across TTLL3 and TTLL8s as in Fig. 4*A*. Arrows indicate TTLL8 residues important for glycylation. Residues D328–D330 are not resolved in our structure (*SI Materials and Methods*); their approximate position is indicated by an arrow. (*B*) Normalized glycylation activity of GFP-tagged wild-type mouse TTLL8 and site-directed mutants as determined by quantifying the glycylation signal from immunofluorescence in U2OS cells (*SI Materials and Methods*; $n \geq 50$ cells for each construct; error bars show SEM; ***$P < 0.001$; ****$P < 0.0001$). (*C*) Sequence alignment of TTLL3 and TTLL8 showing conservation of the IS2 DID motif. Cm, *Chelonia mydas*; Dr, *Danio rerio*; Hs, *Homo sapiens*; Mm, *Mus musculus*; Sc, *Struthio camelus australis*; Xt, *X. tropicalis*. (*D*) Cellular distribution (green) and glycylation activity (red) of GFP-tagged wild type and IS2 mutants transiently transfected in U2OS cells. (Scale bar, 10 μm.) (*D*, *Insets*) (Magnification, 2.5×.)

BIOCHEMISTRY

Both TTLL3 and TTLL8 function in cilia and flagella, cellular structures that are highly enriched in glutamylation (37). Glutamylation is prevalent during ciliogenesis; however, glycylation is required for stabilization of an already-formed cilium (22). Therefore, TTLL3 and TTLL8 likely encounter tubulin that is already glutamylated. We demonstrate with purified components that the glycylase TTLL3 and glutamylase TTLL7 compete for overlapping initiating sites on the β-tail, providing a molecular basis for the observed negative correlation between glutamylation and glycylation in vivo (13, 25, 26, 32). Consistent with this competition, TTLL3 activity is drastically reduced on microtubules with abundant glutamylation. Unexpectedly, we find that at high levels of β-tubulin tail glutamylation, α-tail glycylation by TTLL3 is enhanced. This finding is consistent with prior in vivo studies in *Tetrahymena* showing that removal of glycylation/glutamylation sites in the β-tail enhances α-tail glycylation (26). Although the functional significance of this observation remains to be explored, our study provides a blueprint for investigating how tubulin modification patterns are generated in vivo through the intersection of activities of multiple TTLL enzymes.

Materials and Methods

Protein Production, Crystallization, and Structure Determination. Baculovirus expression clones for wild-type and mutant TTLL3 constructs were generated as described in *SI Materials and Methods*. TTLL3 crystallization and X-ray data collection are described in detail in *SI Materials and Methods*. Detailed procedures for structural determination and refinement are in Table S1 and *SI Materials and Methods*. The structure was solved by molecular replacement using Phaser (43). Iterative rounds of model building in Coot (44) and refinement in PHENIX (45) were performed.

MS/MS Analyses of Glycylated and Glutamylated Peptides. TTLL3 was incubated with Taxol-stabilized unmodified human microtubules, and reactions were prepared for MS/MS analyses as described in *SI Materials and Methods*. A Thermo Fisher Orbitrap Elite mass spectrometer coupled with a 3000 UltiMate HPLC was used for LC/MS/MS data acquisition. Samples were separated as detailed and spectra were analyzed as detailed in *SI Materials and Methods*. TTLL7 was incubated with Taxol-stabilized unmodified microtubules and reactions were prepared for MS/MS analyses as described in *SI Materials and Methods*. Modifications related to [^{13}C]glutamylation were custom-built and searched against. All spectra corresponding to glutamylated peptides were manually curated.

ACKNOWLEDGMENTS. We thank the staff at Sector 5 (Advanced Light Source) for X-ray data collection support, and D.-Y. Lee and the NHLBI Biochemistry Core for access to mass spectrometers. A.R.-M. is supported by the intramural programs of the National Institute of Neurological Disorders and Stroke and National Heart, Lung, and Blood Institute.

1. Roll-Mecak A (2015) Intrinsically disordered tubulin tails: Complex tuners of microtubule functions? *Semin Cell Dev Biol* 37:11–19.
2. Verhey KJ, Gaertig J (2007) The tubulin code. *Cell Cycle* 6:2152–2160.
3. Yu I, Garnham CP, Roll-Mecak A (2015) Writing and reading the tubulin code. *J Biol Chem* 290:17163–17172.
4. Valenstein ML, Roll-Mecak A (2016) Graded control of microtubule severing by tubulin glutamylation. *Cell* 164:911–921.
5. Bieling P, et al. (2008) CLIP-170 tracks growing microtubule ends by dynamically recognizing composite EB1/tubulin-binding sites. *J Cell Biol* 183:1223–1233.
6. Nirschl JJ, Magiera MM, Lazarus JE, Janke C, Holzbaur EL (2016) α-Tubulin tyrosination and CLIP-170 phosphorylation regulate the initiation of dynein-driven transport in neurons. *Cell Reports* 14:2637–2652.
7. Raybin D, Flavin M (1977) Enzyme which specifically adds tyrosine to the alpha chain of tubulin. *Biochemistry* 16:2189–2194.
8. Murofushi H (1980) Purification and characterization of tubulin-tyrosine ligase from porcine brain. *J Biochem* 87:979–984.
9. Schröder HC, Wehland J, Weber K (1985) Purification of brain tubulin-tyrosine ligase by biochemical and immunological methods. *J Cell Biol* 100:276–281.
10. van Dijk J, et al. (2007) A targeted multienzyme mechanism for selective microtubule polyglutamylation. *Mol Cell* 26:437–448.
11. Ikegami K, et al. (2006) TTLL7 is a mammalian beta-tubulin polyglutamylase required for growth of MAP2-positive neurites. *J Biol Chem* 281:30707–30716.
12. Rogowski K, et al. (2009) Evolutionary divergence of enzymatic mechanisms for posttranslational polyglycylation. *Cell* 137:1076–1087.
13. Wloga D, et al. (2009) TTLL3 is a tubulin glycine ligase that regulates the assembly of cilia. *Dev Cell* 16:867–876.
14. Konno A, Setou M, Ikegami K (2012) Ciliary and flagellar structure and function—Their regulations by posttranslational modifications of axonemal tubulin. *Int Rev Cell Mol Biol* 294:133–170.
15. Ishikawa H, Marshall WF (2011) Ciliogenesis: Building the cell's antenna. *Nat Rev Mol Cell Biol* 12:222–234.
16. Redeker V, et al. (1994) Polyglycylation of tubulin: A posttranslational modification in axonemal microtubules. *Science* 266:1688–1691.
17. Bré MH, et al. (1996) Axonemal tubulin polyglycylation probed with two monoclonal antibodies: Widespread evolutionary distribution, appearance during spermatozoan maturation and possible function in motility. *J Cell Sci* 109:727–738.
18. Rüdiger M, Plessmann U, Rüdiger AH, Weber K (1995) Beta tubulin of bull sperm is polyglycylated. *FEBS Lett* 364:147–151.
19. Wall KP, et al. (2016) Molecular determinants of tubulin's C-terminal tail conformational ensemble. *ACS Chem Biol* 11:2981–2990.
20. Ikegami K, Setou M (2009) TTLL10 can perform tubulin glycylation when co-expressed with TTLL8. *FEBS Lett* 583:1957–1963.
21. Rocha C, et al. (2014) Tubulin glycylases are required for primary cilia, control of cell proliferation and tumor development in colon. *EMBO J* 33:2247–2260.
22. Bosch Grau M, et al. (2013) Tubulin glycylases and glutamylases have distinct functions in stabilization and motility of ependymal cilia. *J Cell Biol* 202:441–451.
23. Forrest WF, Cavet G (2007) Comment on "The consensus coding sequences of human breast and colorectal cancers." *Science*, 10.1126/science.1138179.
24. Pathak N, Austin CA, Drummond IA (2011) Tubulin tyrosine ligase-like genes ttll3 and ttll6 maintain zebrafish cilia structure and motility. *J Biol Chem* 286:11685–11695.
25. Kann ML, Prigent Y, Levilliers N, Bré MH, Fouquet JP (1998) Expression of glycylated tubulin during the differentiation of spermatozoa in mammals. *Cell Motil Cytoskeleton* 41:341–352.
26. Redeker V, et al. (2005) Mutations of tubulin glycylation sites reveal cross-talk between the C termini of alpha- and beta-tubulin and affect the ciliary matrix in *Tetrahymena*. *J Biol Chem* 280:596–606.
27. Vemu A, Garnham CP, Lee DY, Roll-Mecak A (2014) Generation of differentially modified microtubules using in vitro enzymatic approaches. *Methods Enzymol* 540:149–166.
28. Widlund PO, et al. (2012) One-step purification of assembly-competent tubulin from diverse eukaryotic sources. *Mol Biol Cell* 23:4393–4401.
29. Jensen-Smith HC, Ludueña RF, Hallworth R (2003) Requirement for the betaI and betaIV tubulin isotypes in mammalian cilia. *Cell Motil Cytoskeleton* 55:213–220.
30. Vinh J, et al. (1999) Structural characterization by tandem mass spectrometry of the posttranslational polyglycylation of tubulin. *Biochemistry* 38:3133–3139.
31. Mary J, Redeker V, Le Caer JP, Rossier J, Schmitter JM (1996) Posttranslational modifications in the C-terminal tail of axonemal tubulin from sea urchin sperm. *J Biol Chem* 271:9928–9933.
32. Bulinski JC (2009) Tubulin posttranslational modifications: A Pushmi-Pullyu at work? *Dev Cell* 16:773–774.
33. Mukai M, et al. (2009) Recombinant mammalian tubulin polyglutamylase TTLL7 performs both initiation and elongation of polyglutamylation on beta-tubulin through a random sequential pathway. *Biochemistry* 48:1084–1093.
34. Redeker V (2010) Mass spectrometry analysis of C-terminal posttranslational modifications of tubulins. *Methods Cell Biol* 95:77–103.
35. Mary J, Redeker V, Le Caer JP, Promé JC, Rossier J (1994) Class I and IVa beta-tubulin isotypes expressed in adult mouse brain are glutamylated. *FEBS Lett* 353:89–94.
36. Geimer S, Teltenkötter A, Plessmann U, Weber K, Lechtreck KF (1997) Purification and characterization of basal apparatuses from a flagellate green alga. *Cell Motil Cytoskeleton* 37:72–85.
37. Schneider A, Plessmann U, Felleisen R, Weber K (1998) Posttranslational modifications of trichomonad tubulins; identification of multiple glutamylation sites. *FEBS Lett* 429:399–402.
38. Garnham CP, et al. (2015) Multivalent microtubule recognition by tubulin tyrosine ligase-like family glutamylases. *Cell* 161:1112–1123.
39. Prota AE, et al. (2013) Structural basis of tubulin tyrosination by tubulin tyrosine ligase. *J Cell Biol* 200:259–270.
40. Szyk A, Deaconescu AM, Piszczek G, Roll-Mecak A (2011) Tubulin tyrosine ligase structure reveals adaptation of an ancient fold to bind and modify tubulin. *Nat Struct Mol Biol* 18:1250–1258.
41. Sjöblom T, et al. (2006) The consensus coding sequences of human breast and colorectal cancers. *Science* 314:268–274.
42. Amanchy R, et al. (2007) A curated compendium of phosphorylation motifs. *Nat Biotechnol* 25:285–286.
43. McCoy AJ, et al. (2007) Phaser crystallographic software. *J Appl Crystallogr* 40:658–674.
44. Emsley P, Cowtan K (2004) Coot: Model-building tools for molecular graphics. *Acta Crystallogr D Biol Crystallogr* 60:2126–2132.
45. Adams PD, et al. (2010) PHENIX: A comprehensive Python-based system for macromolecular structure solution. *Acta Crystallogr D Biol Crystallogr* 66:213–221.
46. Levine RL (2006) Fixation of nitrogen in an electrospray mass spectrometer. *Rapid Commun Mass Spectrom* 20:1828–1830.
47. Perkins DN, Pappin DJ, Creasy DM, Cottrell JS (1999) Probability-based protein identification by searching sequence databases using mass spectrometry data. *Electrophoresis* 20(18):3551–3567.
48. Chen et al. (2010) MolProbity: All-atom structure validation for macromolecular crystallography. *Acta Crystallographica* D66:12–21.
49. Li L, et al. (2012) DelPhi: A comprehensive suite for DelPhi software and associated resources. *BMC Biophys* 5:9.
50. Edelstein A, Amodaj N, Hoover K, Vale R, Stuurman N (2010) Computer control of microscopes using μManager. *Curr Protoc Mol Biol* 92:14.20.1–14.20.17.